

Study of Heat Transfer of Nanofluids in a Circular Tube

M. Amoura, M. Alloti, A. Mouassi, N. Zeraibi

Abstract—Heat transfer behavior of three different types of nanofluids flowing through a horizontal tube under laminar regime has been investigated numerically. The wall of tube is maintained at constant temperature. Al_2O_3 -water, CuO -water and TiO_2 -water are used with different Reynolds number and different volume fraction. The numerical results of heat transfer indicate that the Nusselt number of nanofluids is larger than that of the base fluid. The Pressure loss coefficient decreases by increasing Reynolds number for all types of nanofluids. Results of Nusselt number enhancement and pressure loss coefficient enhancement indicate that Al_2O_3 nanoparticles give the best results in term of thermal-hydraulic properties.

Keywords—Heat transfer, Laminar flow, Nanofluid, Numerical study.

I. INTRODUCTION

THE flow and heat transfer is an important phenomenon in engineering systems due to its wide application in electronic cooling, heat exchangers, double pane windows etc.. The enhancement of heat transfer in these systems is an essential topic from an energy saving perspective. The lower heat transfer performance when conventional fluids, such as water, engine oil and ethylene glycol are used hinders improvements in performance and a consequent reduction in the size of such systems. The use of solid particles as an additive suspended into the base fluid is a technique for heat transfer enhancement [1], [2].

Suspensions of nano-sized (<100nm) particles in conventional heat transfer fluids (such as water, ethylene glycol, and engine oil) were named nanofluid by Choi [3]. To understand and describe various features of flow and heat transfer behavior of nanofluids, numerous investigations have been carried out [4]. Almost all previous investigations show that the thermal conductivity of nanofluids increases significantly over that of the base fluid [4]-[6]

Oxide nanoparticles [7]-[11], carbon nanotubes [12], [13] and other types on nanoparticles [14]-[17] have been used in the preparation of nanofluids. Conventional heat transfer fluids such

F. M. Amoura is with the Université des Sciences et de la technologie Houari Boumedienne, Faculté de Physique, Dépt. Energétique. B.P. 32 El-Alia, 16111 Bab-Ezzouar, Alger, Algeria (phone: +213 21 247 344; fax: +213 21 247 344; e-mail: am_louni@yahoo.fr).

S. M. Alloti, Jr., is with the Université des Sciences et de la technologie Houari Boumedienne, Faculté de Physique, Dépt. Energétique. B.P. 32 El-Alia, 16111 Bab-Ezzouar, Alger, Algeria.

T. A. Mouassi was with the Université de Boumerdes, Faculté des hydrocarbures, Dépt. Transport et Equipements, Avenue de l'indépendance, 35000 Boumerdes, Algeria.

Fo. N. Zeraibi is with the Université de Boumerdes, Faculté des hydrocarbures, Dépt. Transport et Equipements, Avenue de l'indépendance, 35000 Boumerdes, Algeria.

as water, ethylene glycol and transformer oil have been employed as base fluid. All investigators have studied convective heat transfer of nanofluids in circular tubes. Results of these investigations show that the heat transfer coefficient of nanofluids is considerably higher than that of the base fluid and the enhancement of heat transfer coefficient increases with nanoparticle concentration and nanofluid flow rate.

Convective heat transfer characteristics of three different types of nanofluids Al_2O_3 -water, CuO -water and TiO_2 -water in horizontal circular tube with constant wall temperature in the laminar flow regime were studied numerically. A computational code by use of the finite volume method is developed [18]. Laminar model was used to simulate the flow and heat transfer using the SIMPLE scheme for pressure-velocity coupling. This code is validated by comparison with results reported in the literature.

II. PROBLEM FORMULATION

The geometry under investigation is shown in Fig. 1. We consider a horizontal circular tube with a finite length and a diameter D . The flow will be considered as axi-symmetric and therefore it is two dimensional so that it can be represented by the axial and radial coordinates only. The tube contains water and nanoparticles. These particles are assumed to be in the same size and shape. In addition, the solid particles are in thermal equilibrium with the base fluid and they are the same velocity.

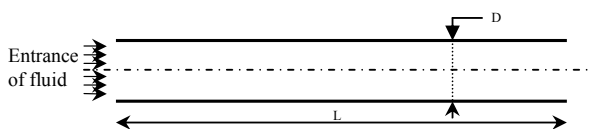


Fig. 1 Geometry of the problem

The physical properties of the nanofluid are assumed to be independent of temperature but of course are functions of the volume fraction ϕ of the suspended nanoparticles. The buoyancy effects are neglected. The thermophysical properties such as density, thermal conductivity of the base fluid and nanoparticle and viscosity are summarized in Table I.

The governing equations for nanofluid in axi-symmetric cylinder are the continuity, momentum, and energy equations with their density, thermal conductivity, and viscosity modified for nanofluid application. The continuity written in cylindrical coordinate for an axi-symmetric geometry is:

$$\frac{\partial(\rho_{nf}u)}{\partial x} + \frac{1}{r} \frac{\partial(\rho_{nf}rv)}{\partial r} = 0 \tag{1}$$

Momentum equations in the axial and radial directions are:

$$\rho_{nf} \frac{\partial(uu)}{\partial x} + \rho_{nf} \frac{1}{r} \frac{\partial(rvu)}{\partial x} - \frac{\partial P}{\partial x} + \frac{\partial}{\partial x} \left(\mu_{nf} \frac{\partial u}{\partial x} \right) + \frac{1}{r} \frac{\partial}{\partial r} \left(r \mu_{nf} \frac{\partial u}{\partial r} \right) \tag{2}$$

$$\rho_{nf} \frac{\partial(uv)}{\partial x} + \rho_{nf} \frac{1}{r} \frac{\partial(rv^2)}{\partial r} - \frac{\partial P}{\partial r} + \frac{\partial}{\partial x} \left(\mu_{nf} \frac{\partial v}{\partial x} \right) + \frac{1}{r} \frac{\partial}{\partial r} \left(r \mu_{nf} \frac{\partial v}{\partial r} \right) - \mu_{nf} \frac{v}{r^2} \tag{3}$$

The axi-symmetric form of energy equation is:

$$\rho_{nf} \frac{\partial(uT)}{\partial x} + \rho_{nf} \frac{1}{r} \frac{\partial(rvT)}{\partial r} - \frac{\partial}{\partial x} \left(\frac{k_{nf}}{c_{p,nf}} \frac{\partial T}{\partial x} \right) + \frac{1}{r} \frac{\partial}{\partial r} \left(r \frac{k_{nf}}{c_{p,nf}} \frac{\partial T}{\partial r} \right) \tag{4}$$

As mentioned before, nanofluid properties are combinations of base fluid and particle properties. The effective density of nanofluid is predicted by mixing theory:

$$\rho_{nf} = \rho_{particle}\phi + \rho_{bf}(1 - \phi) \tag{5}$$

Specific heat is also defined by mixing theory:

$$Cp_{nf} = \frac{\rho_{particle} Cp_{particle} \phi + \rho_{bf} Cp_{bf} (1-\phi)}{\rho_{nf}} \tag{6}$$

TABLE I
MATERIAL PROPERTIES OF FLUID AND NANOPARTICLE [19]-[20]

	Water	CuO	Al ₂ O ₃	TiO ₂
Density (kg/m ³)	1000	6350	3970	4157
Thermal conductivity (W/m K)	0.6	69	36	8.4
Specific heat capacity (J/kg K)	4183	535	765	710
Dynamic viscosity (Ns/m ²) x 10 ⁻³	1.003	-	-	-

The thermal conductivity of nanofluid was evaluated from the model proposed by Maxwell [21] namely:

$$k_{nf} = k_{bf} + 3\phi \frac{k_{particle} - k_{bf}}{k_{particle} + 2k_{bf} - \phi(k_{particle} - k_{bf})} k_{bf} \tag{7}$$

The effective viscosity of fluid containing small particles is given by Brinkman [22] as:

$$\mu_{nf} = \frac{\mu_{bf}}{(1-\phi)^{2.5}} \tag{8}$$

The dimensionless form of the governing equations can be obtained by use of dimensionless variables defined as:

$$U = \frac{u}{u_0} ; P = \frac{p}{\rho u_0} ; R = \frac{r}{D} ; \theta = \frac{T-T_0}{T_{wall}-T_0} \tag{9}$$

The problem is characterized by the following parameters of similarity:

the Reynolds number: $Re = \frac{\rho_{nf}UD}{\mu_{nf}}$ (10)

the Prandtl number: $Pr = \frac{\mu_{nf} Cp_{nf}}{k_{nf}}$ (11)

the Peclet number: $Pe = Re Pr$ (12)

The Nusselt number of the nanofluids is expected to depend on a number of factors such as thermal conductivity and specific heat capacity, the volume fraction of the suspends particles, the flow structure and the viscosity of the nanofluid. The Nusselt number of the nanofluid can be expressed as [23]:

$$Nu = \begin{cases} 1.953 \left(RePr \frac{D}{x} \right)^{\frac{1}{3}} & \left(RePr \frac{D}{x} \right) \geq 33.3 \\ 4.364 + 0.0722 RePr \frac{D}{x} & \left(RePr \frac{D}{x} \right) \leq 33.3 \end{cases} \tag{13}$$

The mean temperature of the fluid for an axi-symmetric case at any cross-section of the tube is:

$$T_{mean} = \frac{\int_0^{D/2} 2\pi\rho C_p T u r dr}{\int_0^{D/2} 2\pi\rho u r dr} = \frac{2}{U_{mean}(D/2)^2} \int_0^{D/2} T(r,x)u(r,x)r dr \tag{14}$$

where T is the temperature at a distance r from the axis where the axial velocity is u .

The boundary conditions in this geometry are summarized in Fig. 2 and Table II.

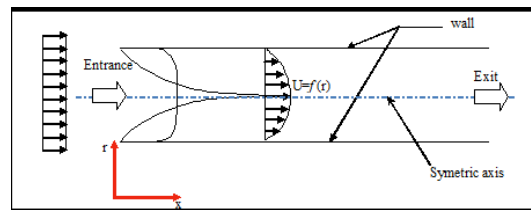


Fig. 2 Boundary conditions

TABLE II
BOUNDARY CONDITIONS

The condition	Entrance	Wall	Symmetric axis
Axial velocity U	$U_0 = \frac{Re\mu}{\rho D}$	$U=0$	$\frac{\partial U}{\partial r} = 0$
Radial velocity V	$V=0$	$V=0$	$V=0$
Temperature T	$T_0=288\text{ K}$	$T=T_{\text{wall}}=320\text{ K}$	$\frac{\partial T}{\partial r} = 0$

The numerical simulation is based on the finite volume formulation. The governing equations are integrated over each control volume to obtain a set of linear algebraic equations. These equations were solved by employing SIMPLE algorithm for the pressure correction processes, and convective and diffusive terms were discretized by upwind and central difference schemes, respectively. Second order discretization scheme were employed for all simulation. For cylinder's diameter less than 10 cm and a length equal to 5 m, a grid independence study was carried out with three different (301x31, 401x31 and 421x31) grid sizes. These studies are performed for 10% volume fraction of CuO. Mean temperature profiles along of the cylinder are plotted for Reynolds number equal at 25 as shown in Fig. 3.

From Fig. 3 it is very clear that grid size 401x31 and 421x31 gave same results. The 401x31 and non-uniform grid is chosen for computation, allowing fine grid spacing near the wall of cylinder (Fig. 4).

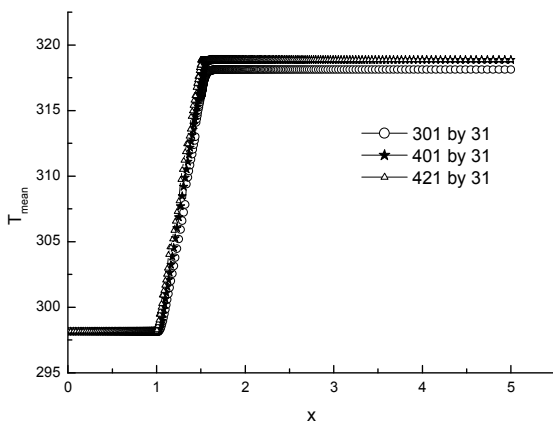


Fig. 3 Temperature profiles at Re=25 for 10% volume fraction of CuO



Fig. 4 Schematic of grid

The convergence of the numerical solution is based on residuals of governing equations that were summed over all cells in the computational domain. Convergence was achieved when the summation of residuals decreased to less than 10^{-8} for all equations.

Furthermore, in order to validate the numerical code used for the present study, the steady-state solutions obtained as

time-asymptotic solutions for an vertical square cavity with differentially heated sidewalls and adiabatic top and bottom walls, have been compared with the results of Hadjisophocleous [24], Tiwari [25] and Kuang [26]. In particular, the average Nusselt numbers, the maximum horizontal and vertical velocity components obtained at Rayleigh numbers in the range between 10^3 and 10^6 are summarized in the Table III. A very agreement has been obtained.

TABLE III
COMPARISON BETWEEN PRESENT STUDY AND RESULTS REPORTED IN THE LITERATURE

	Hadjisophocleous[24]	Tiwari [25]	Kuang [26]	Present study
$Ra=10^3$				
u_{max}	3.544	3.642	3.597	3.643
Y	0.814	0.804	0.819	0.818
v_{max}	3.586	3.702	3.669	3.690
X	0.186	0.178	0.181	0.179
\bar{Nu}	1.141	1.087	1.118	1.108
$Ra=10^4$				
u_{max}	15.995	16.144	16.185	16.164
Y	0.814	0.822	0.819	0.821
v_{max}	18.894	19.665	19.648	19.665
X	0.103	0.110	0.112	0.111
\bar{Nu}	2.29	2.195	2.243	2.228
$Ra=10^5$				
u_{max}	37.144	34.30	36.732	36.720
Y	0.855	0.856	0.858	0.857
v_{max}	68.91	68.77	68.288	68.260
X	0.061	0.059	0.063	0.060
\bar{Nu}	4.964	4.450	4.511	4.489
$Ra=10^6$				
u_{max}	66.42	65.59	66.47	66.48
Y	0.897	0.839	0.869	0.890
v_{max}	226.4	219.73	222.34	219.55
X	0.0206	0.04237	0.03804	0.0399
\bar{Nu}	10.39	8.803	8.758	8.765

III. RESULTS

The heat transfer performance has been investigated for the Reynolds number range $25 < Re < 600$ and for different volume fractions. The temperature, the Nusselt number and the pressure loss coefficient profiles are presented for the different cases.

Fig. 5 represents variation of mean Nusselt number with Reynolds number at different nanoparticle volume fractions (0%, 1%, 2%, 3% and 10%) and for different kind of nanofluids. We have seen that addition of nanoparticles to the base fluid enhances its heat transfer significantly. Also, for Re greater than 400, Nusselt number is a increasing function of Reynolds number for all nanfluids.

In Fig. 6, we observe that at Re=600, the curve giving the evolution of Nusselt number as function of volume fraction is independent of the other curves. We can explain this by the fact that the thermal developed regime is not yet reached.

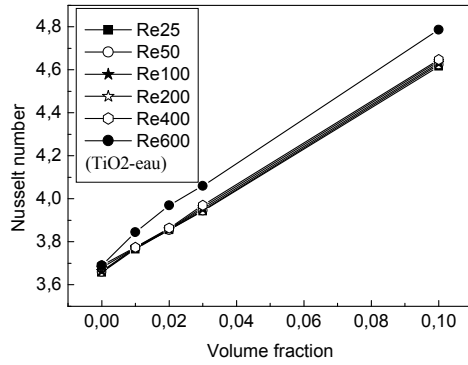
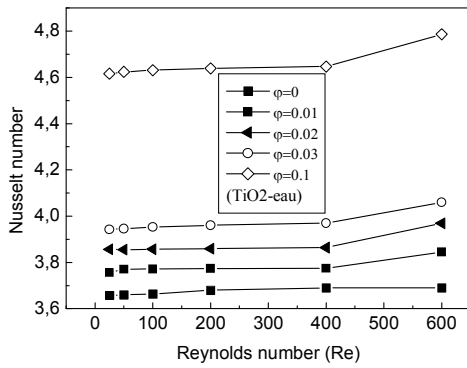
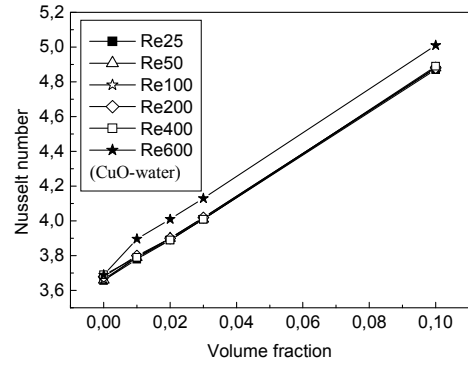
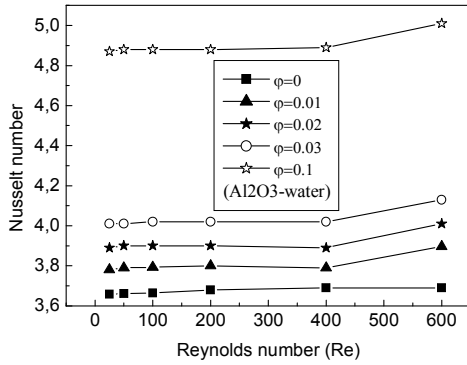
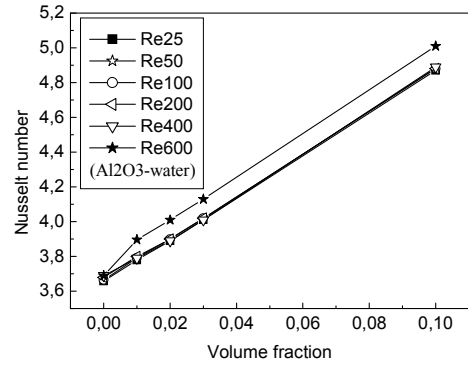
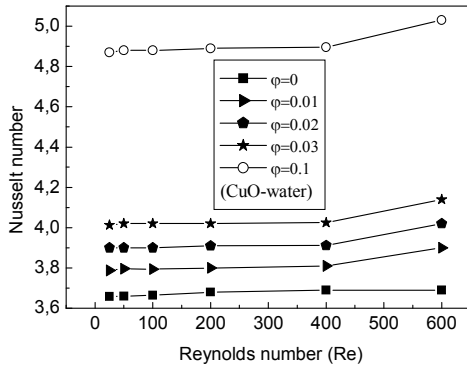


Fig. 5 Nusselt number for different particle volume fraction and different nanofluids as a function of Reynolds number

Fig. 6 Nusselt number for different Reynolds number and different nanofluids as a function of particle volume fraction

In order to show the importance of the different kinds of nanoparticle in the water on heat transfer, we have calculated the Nusselt number enhancement by the following equation:

$$Nu(\%) = \frac{Nu_{nf} - Nu_{water}}{Nu_{water}} \quad (15)$$

The values of the Nusselt number enhancement at two given Reynolds number for different kinds of nanofluid and different volume fraction are summarized in Tables IV and V. The highest heat transfer was obtained for CuO-water nanofluid.

TABLE IV
NUSSELT NUMBER ENHANCEMENT (Nu%) AT Re=25

Taux	φ=0.01	φ=0.02	φ=0.03	φ=0.1
Al ₂ O ₃	3.55	6.55	9.56	33.33
Cuo	3.72	6.55	9.83	33.33
TiO ₂	3.024	5.327	7.797	26.33

TABLE V
 NUSSELT NUMBER ENHANCEMENT (Nu%) AT Re=600

Taux	$\phi=0.01$	$\phi=0.02$	$\phi=0.03$	$\phi=0.1$
Al ₂ O ₃	5.59	8.672	11.924	35.772
Cuo	5.69	8.94	12.195	36.314
TiO ₂	4.19	7.57	10.027	29.718

We observe a considerable increasing for the Nusselt number enhancement comparatively to the water (Fig. 7).

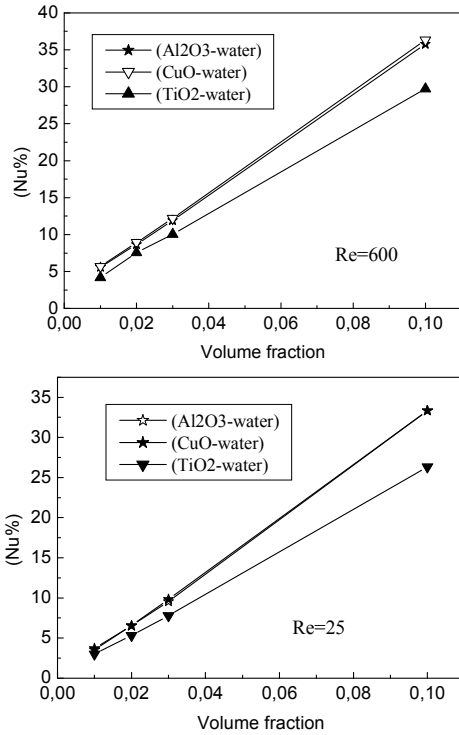


Fig. 7 Nusselt number enhancement for different nanofluids as a function of particle volume fraction

A comparison of the bulk temperature evolution with Reynolds number at different kind of nanofluids is shown in Fig. 8. At given volume fraction ($\phi=10\%$), this figure shows that the CuO-water nanofluid gives the highest bulk temperature.

Fig. 9 illustrates the pressure loss coefficient as a function of Reynolds number for different kind of nanofluids and for particle volume fraction $\phi=10\%$. Unfortunately, the figure shows that for CuO-water nanofluid, the pressure loss coefficient is more important than for the Al₂O₃-water nanofluid and TiO₂-water nanofluid. Despite of this, the CuO-water nanofluid gives a best heat transfer enhancement.

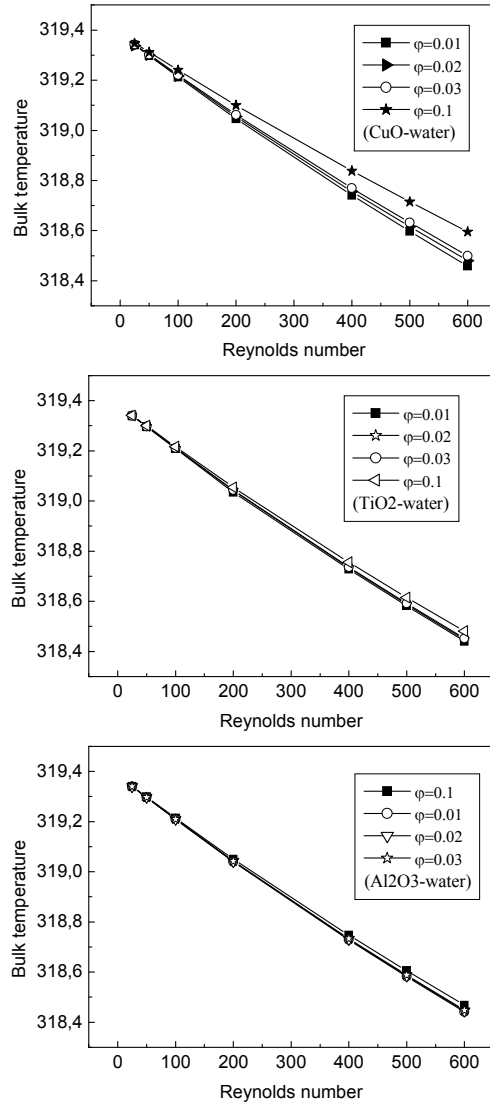


Fig. 8 Bulk temperature for different nanofluids and different particle volume fraction as a function of Reynolds number

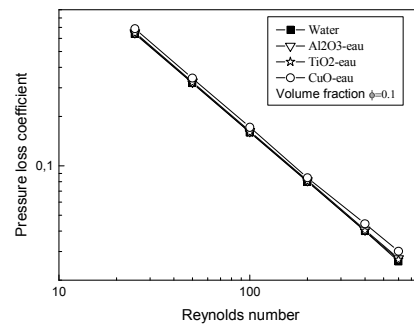


Fig. 9 Pressure loss coefficient for different nanofluids at particle volume fraction $\phi=10\%$ as a function of Reynolds number

In order to determine which kind of nanoparticle has the best thermal-hydraulic properties, we have also calculated the pressure loss coefficient enhancement by the following equation:

$$\lambda(\%) = \frac{\lambda_{nf} - \lambda_{water}}{\lambda_{water}} \quad (16)$$

The values of the pressure loss coefficient enhancement for different particle volume fraction and for different kind of nanofluids are summarized in Table VI. We note that the Al₂O₃ nanoparticle gives the small value of pressure loss coefficient.

Taux	$\varphi=0.01$	$\varphi=0.02$	$\varphi=0.03$	$\varphi=0.1$
Al ₂ O ₃	0.11	0.66	0.7	1.75
Cuo	1.78	3.31	4.21	10.96
TiO ₂	0.23	2.13	3.21	1.75

IV. CONCLUSION

The effect of using different nanofluids on the heat transfer in a horizontal cylinder was studied numerically for a range of Reynolds numbers and nanoparticles volume fraction.

Indeed, the results revealed that the suspended nanoparticles increase the heat transfer with an increase in the nanoparticles volume fraction and at any given Reynolds number. The results show the influence of nanoparticles on the pressure drop and we identified the kind of nanoparticle that gives better heat transfer and a minimum pressure drop.

NOMENCLATURE

Cp	Specific heat (J/kg K)	Greek symbols
D	Diameter (m)	ϕ Nanoparticle volume fraction
L	Length of cylinder (m)	μ Dynamic viscosity (kg/m s)
q	Heat flux (W/m ²)	ρ Density (kg/m ³)
Re	Reynolds number	Subscripts
r	Radius	f fluid
T	Temperature	nf nanofluid
u, v	Velocity components	bf base fluid
x, r	Axial and radial coordinates	

REFERENCES

- [1] S.U.S. Choi, Z.G. Zhang, W. Yu, F.E. Lockwood and E.A. Grulke, "Anomalous thermal conductivity enhancement in nano-tube suspensions", *Applied Physics Letters*, No. 79 2001, pp 2252–2254.
- [2] S.K. Das, N. Putta, P. Thiesen and W. Roetzel, "Temperature dependence of thermal conductivity enhancement for nanofluids", *ASME Trans. J. Heat Transfer*, No. 125, 2003, pp 567–574.
- [3] S.U.S. Choi, "Developments and Applications of Non-Newtonian Flows", *Fluids Engineering Division FED*, No. 231, 1995, pp 99-112.
- [4] L. Godson, B. Raja, D. Mohan and S. Wongwises, "Enhancement of heat transfer using nanofluids", *Renew. Sustainable Energy Rev.*, Vol. 14, No2, 2009, pp 629-641.
- [5] Y. Li, J. Zhou, S. Tung, E. Schneider and S. Xi, "A review on development of nanofluid preparation and characterization", *Powder Technol.*, Vol. 196, No 2, 2009, pp 89-101.
- [6] W. Yu, D. M. France, J.L. Routbort and S.U.S. Choi, "Review and comparison of nanofluid thermal conductivity and heat transfer enhancement", *Heat transf. Eng.*, Vol. 29, No 5, 2008, pp 432-460.
- [7] B.C. Pak. and Y. I. Cho, "Hydrodynamic and heat transfer study of dispersed fluids", *Int. J. Heat Mass Transf.*, Vol. 11, 1998, pp 5181-5201.
- [8] D. Wen and Y. Ding, "Experimental investigation into convective heat transfer of nanofluids at the entrance region under laminar flow conditions", *Int. J. Heat Mass Transfer*, No. 47, 2004, pp 5181–5188.
- [9] S. Z. Heris, S. G. Etemad and M. N. Esfahany, "Experimental investigation of oxide nanofluids laminar flow convective heat transfer", *Int. Commun. Heat Mass Transf.*, Vol. 33, No 4, 2006, pp 529-535.
- [10] Y. He, Y. Jin, H. Chen, Y. Ding, D. Cang and H. Lu, "Heat transfer and flow behaviour of aqueous suspensions of TiO₂ nanoparticles", *Int. J. Heat Mass Transf.*, Vol. 50, No 11, 2007, pp 2272-2281.
- [11] C.T. Nguyen, G. Roy, C. Gauthier and N. Galaris, Heat transfer enhancement using Al₂O₃ water nanofluid for an electronic liquid cooling system, *App. Therm. Eng.*, Vol. 27, No 8, 2007, pp 1501-1506.
- [12] Y. Ding, H. Alias, D. Wen and R. A. Williams, Heat transfer of aqueous suspensions of Carbon nanotubes, *Int. Commun. Heat Mass Transf.*, Vol. 49, 2006, pp 240-250.
- [13] P. Garg, J.L. Alvarado, C. Marsh, T.A. Carlson, D.A. Kessler and K. Annamalai, "An experimental study on the effect of ultrasonication on viscosity and heat transfer performance of multiwall carbon nanotube-based aqueous nanofluids", *Int. J. Heat Mass Transf.*, Vol 52, No 21, 2009, pp 5090-5101.
- [14] Y. Xuan and Q. Li, "Investigation on convective heat transfer and flow features of nanofluids", *Int. J. Heat Mass Transfer*, Vol. 125, 2003, pp 151-155.
- [15] Y. Yang, Z.G. Zhang, E.A. Grulke, W.B. Anderson and G. Wu, "Heat transfer properties of nanoparticle in fluid dispersions", *Int. J. Heat Mass Transfer*, Vol. 48, No. 6, 2005, pp 1107-1116.
- [16] W. Yu, D. M. France, D. S. Smith, E. V. Timofeeva and J.L. Routbort, "Heat transfer to a Silicon Carbide/water nanofluid", *Int. J. Heat Mass Transfer*, Vol. 52, No. 15, 2009, pp 3606-3612.
- [17] S. Torii and W. J. Yang, "Heat transfer augmentation of aqueous suspensions of nano-diamonds in turbulent pipe flow", *J. Heat Transf.*, Vol. 131, 2009, pp 1-5.
- [18] S.V. Patankar, "Computation of Conduction and Duct Flow Heat Transfer", Hemisphere Publishing Corporation, New York 1988.
- [19] S.P. Jang and S.U.S. Choi, "Effects of various parameters on nanofluid thermal conductivity", *ASME J. Heat Transfer*, No 129, 2007, pp 617-623.
- [20] E. Abu-Nada, Z. Masoud, H. Oztop and A. Campo, "Effect of nanofluid variable properties on natural convection in enclosures", *Int. J. Thermal Sci.*, No 49, 2010, pp 479-491.
- [21] J. C. Maxwell, "Treatise on Electricity and Magnetism", *Oxford: Clarendon Press* 1873.
- [22] H. Brinkman, "The viscosity of concentrated suspensions and solutions", *J. Chem. Phys.*, No. 20, 1952, pp. 571-581.
- [23] R.K. Shah, "Thermal entry length solutions for the circular tube and parallel plates", *Proceedings of 3rd National Heat and Mass Transfer Conference*, vol. 1, Indian Institute of Technology, Bombay, 1975, p. HMT-11-75.
- [24] G. V. Hadjisophocleous, and J. E. S. Venart, "Predicting the transient natural convection in enclosures of arbitrary geometry using a nonorthogonal numerical model", *Numer. Heat Transfer A*, No. 13, 1998, pp 373–392.
- [25] R.K. Tiwari and M.K. Das, "Heat transfer augmentation in a two-sided lid-driven differentially heated square cavity utilizing nanofluids", *Int. J. Heat Mass Transfer*, No. 50, 2007, pp 2002–2018.
- [26] C.L. Kuang and A. Violi, "Natural convection heat transfer of nanofluids in a vertical cavity: Effects of non-uniform particle diameter and temperature on thermal conductivity.", *Int. J. Heat and Fluid Flow*, No. 31, 2010, pp 236–245.